A Vesicular Stomatitis Virus Recombinant Expressing Granulocyte-Macrophage Colony-Stimulating Factor Induces Enhanced T-Cell Responses and Is Highly Attenuated for Replication in Animals

Elizabeth Ramsburg,[1] Jean Publicover,[1,2] Linda Buonocore,[1] Amanda Poholek,[1] Michael Robek,[1] Amy Palin,[1] and John K. Rose[1]*

Department of Pathology[1] and Section of Microbial Pathogenesis,[2] Yale University School of Medicine, New Haven, Connecticut 06510

Live attenuated vectors based on recombinant vesicular stomatitis viruses (rVSVs) expressing foreign antigens are highly effective vaccines in animal models. In this study, we report that an rVSV (VSV-GMCSF1) expressing high levels of murine granulocyte-macrophage colony-stimulating factor (GM-CSF) from the first position in the viral genome is highly attenuated in terms of viral dissemination and pathogenesis after intranasal delivery to mice. However, this highly attenuated virus generated antibody and T-cell responses equivalent to those induced by a control virus expressing enhanced green fluorescent protein (EGFP) from the first position (VSV-EGFP1). The better containment and clearance of VSV-GMCSF1 may be due to enhanced recruitment of macrophages to the site of infection but is not explained by a greater induction of interferons. The primary CD8 T-cell and neutralizing antibody responses to VSV-GMCSF1 were equivalent to those generated by VSV-EGFP1, while the CD8 T-cell memory and recall responses to the vector were enhanced in mice infected with VSV-GMCSF1. It is likely that the GM-CSF produced by immunization with this virus results in an enhanced recruitment of antigen-presenting cells, leading to better acute and long-term T-cell responses. This recruitment appears to cancel out any negative effect of viral attenuation on immunogenicity.

Recombinant vesicular stomatitis viruses (rVSVs) expressing appropriate foreign antigens have been used to generate experimental vaccines protecting against infection or disease caused by several viral pathogens (27, 29, 30, 33). Although no pathogenesis was observed in nonhuman primates given live attenuated VSV vectors by the oral, intranasal, and intramuscular routes (5, 27, 31), it is likely that additional specific attenuating mutations will be required before live VSV vectors can be used in human vaccine trials. The attenuation of vector pathogenesis is often associated with a loss of immunogenicity, and a loss of immunogenicity was already reported when VSV vectors attenuated for growth were delivered intranasally (25, 29). For the present study, we sought a means of attenuating VSV pathogenesis while simultaneously retaining or enhancing immunogenicity.

rVSVs derived from plasmid DNA are attenuated to the point that they do not cause neuropathogenesis in 6- to 8-week-old mice after intranasal delivery, but still cause transient weight loss (29). Weight loss is a sensitive measure of pathogenesis correlating with the extent of viral replication after intranasal inoculation. We have previously tested immune responses to rVSV vectors in which the VSV G gene has been deleted. These VSVΔG vectors are capable of only a single round of replication in the host and induce strong CD8 T-cell responses when delivered intramuscularly, but they are

much less effective when delivered by the intranasal route (Publicover et al., unpublished data). In contrast, replication-competent rVSVs delivered intranasally generate cytotoxic T-lymphocyte (CTL) responses that are nearly indistinguishable from those generated by intramuscular immunization. These results indicated that more than one round of viral replication is important to the induction of cellular immune responses after intranasal immunization.

The addition of foreign genes to VSV often results in some degree of attenuation of viral growth in culture. In our experience, foreign genes inserted at the extreme 3' position (position 1) in the VSV genome cause the greatest degree of attenuation, probably because of the sequentially attenuated process of VSV transcription. In these recombinants, the foreign gene becomes the most highly expressed one since it is transcribed first and not subject to the transcription attenuation of upstream genes (9). It also attenuates the expression of all downstream VSV genes. In the studies reported here, we hypothesized that high-level expression of the granulocyte-macrophage colony-stimulating factor (GM-CSF) gene in an rVSV vector might result in a less pathogenic vector that could induce enhanced immune responses. GM-CSF is a cytokine responsible for the recruitment, activation, and maturation of antigen-presenting cells (APC) (8). Specifically, it has been reported to increase phagocytosis and gamma interferon (IFN-γ) production by pulmonary macrophages and is necessary for the clearance of multiple viral and bacterial pathogens in the lung (1, 23, 36). Additionally, GM-CSF has been used extensively as a vaccine adjuvant in a variety of plasmid DNA immunizations, where it has been shown to significantly en-

* Corresponding author. Mailing address: Department of Pathology, Yale University School of Medicine, 310 Cedar St. (LH302), New Haven, CT 06510. Phone: (203) 785-6794. Fax: (203) 785-7467. E-mail: john.rose@yale.edu.

hance humoral and CD4 T-cell responses (2, 22). While the stimulatory effect of GM-CSF on CD8 T-cell responses is less well characterized, two groups have demonstrated enhanced CD8 T-cell responses following plasmid vaccination for malaria (40) and DNA prime-poxvirus boost vaccination for vaccinia (35).

We report here that the addition of GM-CSF to a VSV vaccine vector attenuates the vector in terms of host pathogenesis but does not reduce cellular or humoral immune responses. In addition, memory CD8 T-cell responses in mice immunized with VSV expressing GM-CSF were increased relative to those seen in control animals, indicating that the expression of GM-CSF has long-lasting effects on T cells generated during the initial infection. The mechanism by which GM-CSF attenuates VSV-associated pathogenesis likely involves the rapid recruitment of pulmonary macrophages, which in turn promote efficient T-cell priming as well as viral clearance. Most importantly, the immunostimulatory properties of GM-CSF, notably its induction of APC maturation, may counteract the effects of viral attenuation, resulting in a balance between attenuation and immunogenicity.

MATERIALS AND METHODS

Construction of plasmids and recovery of recombinant viruses. A plasmid vector (pVSV1XN) allowing the expression of foreign genes from the first position of the VSV genome was constructed as follows. First, a subclone of the full-length VSV infectious clone (pVSVXN2) (34) suitable for in vitro mutagenesis was generated by digestion with EcoRV and ApaI, trimming with T4 DNA polymerase, and religation. This treatment removed 9,126 bp from the infectious clone and left a plasmid of 5,225 bp lacking the M, G, and L genes. This subclone was used as a template for in vitro mutagenesis to insert a new VSV transcription unit upstream of the VSV N gene. Quick-change mutagenesis was performed according to the manufacturer's instructions (Invitrogen), using two complementary 103-mer oligonucleotides that inserted 53 nucleotides upstream of the N gene. The sequence of the plus-sense primer was 5′-CAGGAGAAACTTTAA CAGTA**ATCAAACTCGAG**GCGCGTCGAGAATTAATT**GCTAGC**TATG AAAAAAAACTAACAGATATCATGTCTGTTACAGTCAAGAGAATC-3′. The minus-sense primer was the exact complement. Mutagenesis introduced the underlined 53 nucleotides just before the ATG translation initiation codon for VSV N and contained XhoI and NheI restriction sites (shown in bold) for the introduction of foreign genes. The N gene transcription start site, AACAGT AAATCAAA, was thus placed upstream of these restriction sites, and a new transcription termination site, TATGAAAAAAA, was introduced downstream of these sites. In addition, mutagenesis introduced a new transcription start site (AACAGATATC) just before the ATG initiation codon of the N gene. This plasmid was digested with BsaA1 and BstZ171. The 1,501-nucleotide fragment containing the new promoter was then cloned into pVSVFL (12) from which the BsaA1/BstZ171 fragment had been removed and the downstream NheI site had been removed. The resulting plasmid with the new transcription unit was designated pVSV1XN.

To obtain a plasmid that could be used to recover an rVSV expressing murine GM-CSF (mGM-CSF) from the first position in the VSV genome, a 503-bp DNA fragment encoding mGM-CSF was amplified from pORF mGM-CSF (Invivogen), using the forward primer 5′-CCCGGG**CTCGAG**ACCATGTAC AGGATGCAACTCCTGTC-3′ and the reverse primer 5′-ATTAAGAGTGGG GTGGCAGG-3′. The forward primer introduced the underlined XhoI site upstream of the GM-CSF coding sequence. The PCR product was digested with XhoI and NheI, purified, and ligated into the pVSV1XN vector, which had been digested with the same enzymes to generate pVSV1XN-GMCSF. We also generated pVSV1XN-EGFP, which was then used to recover an rVSV expressing enhanced green fluorescent protein (EGFP) from the first position of the genome. The 720-bp EGFP gene was amplified from plasmid pEGFP-1, using the forward primer 5′-GGGCCC**CTCGAG**ACCATGGTGAGCAAGGGCGAG GAGC-3′ and the reverse primer 3′-GATCCCCCCGGG**GCTAGC**TTACTTGTAC AGCTCGTCCATGCC-5′. These primers introduced the underlined XhoI and NheI sites upstream and downstream of the EGFP coding sequence, respectively, for cloning into pVSV1XN. Plasmids were recovered after the transformation of *Esch-*

erichia coli and were purified using a Maxi kit (QIAGEN). The insert sequences were verified (Yale Keck Sequencing Facility). Recombinant viruses were recovered from these plasmids as described previously. Briefly, BHK-21 cells were grown to 50% confluence and infected at a multiplicity of infection (MOI) of 10 with vTF7-3, a vaccinia virus expressing T7 RNA polymerase. One hour after infection, cells were transfected with 10 μg of pVSV1XN-GMCSF or pVSV1XN-EGFP along with 3 μg of pBS-N, 5 μg of pBS-P, 1 μg of pBS-L, and 4 μg of pBS-G. While pBS-G is not required for the recovery of recombinants, it was included to enhance the efficiency. After 48 h, cell supernatants were passaged onto BHK-21 cells through a 0.2-μm filter, and medium containing virus was collected about 24 h after the cytopathic effect was seen. Viruses grown from individual plaques were used to prepare stocks that were grown on BHK-21 cells and stored at −80°C. Indirect immunofluorescence staining and microscopy confirmed VSV G and mGM-CSF expression in cells infected with the recombinant. BHK cells on coverslips were infected with virus at an MOI of 10. After 4 to 5 h, cells were fixed with 3% formaldehyde and incubated with mouse monoclonal antibodies I1 and I14 to VSV G followed by a fluorescein isothiocyanate-conjugated goat anti-mouse antibody to confirm VSV G expression. Separate coverslips were incubated with phycoerythrin (PE)-conjugated rat anti-mouse GM-CSF. The expression of abundant EGFP by VSV-EGFP1 was confirmed by fluorescence microscopy.

Metabolic labeling and SDS-PAGE of cells infected with recombinants. BHK cells (10^6) were infected at an MOI of 20 with VSV recombinants. After 5 h, the medium was removed and cells were washed twice with methionine-free Dulbecco's modified Eagle's medium (DMEM). Methionine-free DMEM (1 ml) containing 100 μCi of [^{35}S]methionine was added to each plate for two additional hours. The medium was removed, and cells were washed with phosphate-buffered saline (PBS), lysed with 500 μl of detergent solution (1% Nonidet P-40, 0.4% deoxycholate, 50 mM Tris-HCl [pH 8], 62.5 mM EDTA) on ice for 5 min, and collected into 1.5-ml Eppendorf tubes. The protein extracts were centrifuged for 2 min at 16,000 × g to remove the nuclei and then stored at −20°C. Protein extracts were fractionated by sodium dodecyl sulfate-polyacrylamide gel electrophoresis (SDS-PAGE; 15% acrylamide), and proteins were visualized by autoradiography.

ELISA assay for GM-CSF. BHK cells (10^6 cells/dish) were infected at an MOI of 5 with either VSV-GMCSF1 or VSV-EGFP1. The virus was adsorbed to cells for 1 h, the inoculum was removed and replaced with 1 ml of 5% DMEM, and the infection was allowed to continue. Medium was collected from the cells, and cell lysates were prepared following detergent lysis of cells 0, 4, and 8 h after infection. Cell lysates or media were assayed over a range of dilutions for GM-CSF, using a mouse GM-CSF enzyme-linked immunosorbent assay (ELISA) set (BD OptEIA; BD Biosciences) according to the manufacturer's protocol.

Inoculation of mice. Six-week-old female C57BL/6 mice were obtained from Jackson Laboratories and housed for at least 1 week before experiments were initiated. Mice were housed in microisolator cages in a biosafety level 2-equipped animal facility. Viral stocks were diluted to appropriate titers in serum-free DMEM. For intramuscular vaccination, mice were injected with 5 × 10^5 PFU of virus in 50 μl. For intranasal vaccination, mice were lightly anesthetized with methoxyflurane (Metafane; Medical Developments Australia Pty. Ltd.) and administered 5 × 10^5 PFU of virus in a 25-μl volume. The Institutional Animal Care and Use Committee of Yale University approved all animal experiments.

Preparation of organs for viral titers and RNA extraction. Mice were euthanized via an anesthetic overdose. Immediately after death, the right atrium was nicked and organs were perfused with sterile PBS via the left ventricle. Organs were removed, weighed, and frozen in liquid nitrogen. To obtain suspensions for titration, organs were thawed and disrupted in a Dounce homogenizer in five times their volume of PBS. Suspensions were centrifuged for 5 min at 10,000 × g to remove solids, and the resulting supernatants were divided into aliquots and frozen at −80°C. For titration, samples were thawed, diluted, and plated on semiconfluent BHK-21 cells. Plaques were visualized after 48 h by staining with crystal violet. Organs from which RNAs were prepared were removed after perfusion and immediately frozen in liquid nitrogen. After storage at −80°C, the tissue was homogenized in a guanidine isothiocyanate-containing buffer, and total RNA was prepared using an RNeasy mini kit according to the manufacturer's recommendations (QIAGEN).

Tetramer assay. Splenocytes were obtained by disrupting spleens between the frosted ends of two microscope slides. Red blood cells were removed using red blood cell lysing buffer (Sigma). To obtain lymphocytes from lungs, mice were perfused with sterile PBS until the lungs were cleared of blood. The lungs were removed, chopped into fine pieces, and digested for 2 h at 37°C in DMEM containing 5% fetal calf serum (FCS), 150 U/ml collagenase, and 20 μg/ml DNase. After digestion, the cells were pushed through a metal sieve, filtered, and layered onto a Ficoll gradient. Gradients were spun, and lymphocytes were

collected from the interface. Cells were washed and resuspended in DMEM containing 5% FCS. Staining was performed on freshly isolated lymphocytes as previously described (6). Briefly, approximately 5×10^6 cells were added to the wells of a 96-well V-bottomed plate and blocked with unconjugated streptavidin (Molecular Probes) and Fc block (Pharmingen) for 15 min at room temperature. Following a 5-min centrifugation at $500 \times g$, splenocytes were labeled with a fluorescein isothiocyanate-conjugated anti-CD62L antibody, (Pharmingen), an allophycocyanin-conjugated anti-CD8 antibody (Pharmingen), and a tetramer for 30 min at room temperature. The tetramer was a PE-conjugated major histocompatibility complex (MHC) class I D^d tetramer (generously provided by Leo Lefrancois) containing the VSV N peptide (N-RGYVYQGL-C). CD8 T cells which were tetramer positive and activated (CD62L^{lo}) were identified. Animals vaccinated with rVSV were used to determine the background levels of tetramer binding. The background was routinely <0.1% and was subtracted from all reported percentages.

RT and real-time PCR analysis. One microgram of total RNA was reverse transcribed using random hexamer primers and a Taqman reverse transcription (RT) kit (Applied Biosystems) according to the manufacturer's instructions. RNAs were obtained either from organs harvested from immunized mice or from a hepatocyte cell line used as a reporter for IFN gene induction (24). Real-time PCR was performed in a 25-μl reaction containing 5 μl of reverse transcribed product with 12.5 μl of SybrGreen PCR master mix (Applied Bioscience) and 5 μM (each) forward and reverse primers. To normalize cDNA quantities, a glyceraldehyde-3-phosphate dehydrogenase (GAPDH) control was run with all samples in parallel with the experimental gene. The PCR primers for GAPDH were GAPDH sense (5′-TCTGGAAAGCTGTGCCGTG-3′) and GAPDH antisense (5′-CCAGTGAGCTTCCCGTTCAG-3′). The PCR primers for quantitation of IFN-inducible genes were ISG15 sense (5′-CAATGGCCT GGGACCTAAA-3′), ISG15 antisense (5′-CTTCTTCAGTTCTGACACCGT CAT-3′), OAS sense (5′-GATGTCAAATCAGCCGTCAA-3′), OAS antisense (5′-AGTGTGGTGCCTTTGCCTGA-3′), TGTP sense (5′-CAGCCCACAAGC GTCA-3′), and TGTP antisense (5′-TGGAATGGTGGCTAATGCTC-3′). Quantitative PCR was performed on a thermocycler (Applied Biosystems model 7500) with the following cycling program: 50°C for 2 min, 95°C for 10 min, and a 50-cycle repeat of 95°C for 30 s and 60°C for 1 min. Relative gene expression was determined using software provided by Applied Biosystems. Gene induction in infected animals was expressed as fold induction above that present in uninfected control mice.

IFN-α ELISA. The interferon ELISA protocol was adapted from a previously published assay (14). Briefly, a 96-well flat-bottomed plate was coated with monoclonal antibody (MAb) F-18 (HyCult Biotechnology) in carbonate buffer overnight at 4°C. The plate was washed three times with wash buffer (0.5% Tween in PBS) and blocked in 10% FCS–PBS for 2 h at room temperature. After being blocked, the plate was washed, and bronchoalveolar lavage (BAL) samples were serially diluted in blocking buffer. A recombinant mouse IFN-α (HyCult Biotechnology) was used as a standard at 2,000 pg/ml to 2 pg/ml. Samples were incubated overnight at 4°C. Following overnight incubation, plates were washed and incubated with polyclonal rabbit anti-mouse IFN-α (PBL Biomedical Laboratories) diluted 1:1,000 in blocking buffer for 1 h at room temperature. The plates were washed five times with wash buffer and incubated with horseradish peroxidase-conjugated donkey anti-rabbit F(ab′)$_2$ (Jackson ImmunoResearch Laboratories) for 1 h at room temperature. Following horseradish peroxidase incubation, the plate was washed 10 times with wash buffer. The colorimetric analysis used was 2,2′-azinobis (3-ethylbenzothiazoline-6-sulfonic acid) diammonium salt tablets at 10 mg/tablet (Immunopure ABTS; Pierce) absorbed in 10 ml substrate buffer (1 M acetate buffer, 0.05% Tween 20, pH 4.2). Plates were read for 415-nm absorbance in a Bio-Rad ELISA plate reader.

Bronchoalveolar lavage and cell isolation. Mice were sacrificed via an anesthetic overdose. Immediately after death, the trachea was exposed and cannulated, and lungs were flushed with two injections of 900 μl of sterile PBS to give a total volume of approximately 2 ml BAL fluid. The fluid was collected and placed on ice. Samples were centrifuged at $1,000 \times g$ for 5 min to pellet cells, and then fluid (minus cells) was collected, UV irradiated (to inactivate virus), and frozen at −80°C until use. Cells were transferred to a 96-well plate and stained immediately with antibodies labeling CD11b, CD11c, and CD3.

RESULTS

Expression of murine GM-CSF from recombinant VSV. To obtain a VSV recombinant expressing high levels of GM-CSF, we inserted the 0.5-kb cDNA encoding mGM-CSF into the plasmid vector pVSV1XN. This allowed the recovery of a virus

(VSV-GMCSF1) (Fig. 1A) expressing GM-CSF from the first transcribed gene in the genome, a site which allows maximal mRNA expression. Downstream gene transcription in VSV is attenuated ~30% at each subsequent gene junction during the sequential transcription process (9). The expression of GM-CSF in cells infected with VSV-GMCSF1 was initially verified by metabolic labeling with [^{35}S]methionine, SDS-PAGE, and autoradiography (Fig. 1B). The predicted molecular weight of GM-CSF is approximately 18,500, including the two N-linked glycans. In cells infected with VSV-GMCSF1, we detected the indicated VSV proteins as well as a new protein band with the mobility expected for GM-CSF. This band was absent in lysates from cells infected with rVSV. GM-CSF contains two predicted sites for N-linked glycosylation. To determine if the putative GM-CSF band contained N-linked glycans, we digested the lysates with endoglycosidase F to remove N-linked glycans. This treatment resulted in the disappearance of the putative GM-CSF band and the appearance of a new band with a faster mobility (Fig. 1B), consistent with the removal of the two N-linked glycans. We also observed the expected shift in the mobility of the VSV G protein due to the removal of its two glycans. Although the band of GM-CSF protein appears weak relative to those of the VSV proteins, this is due to the fact that mature GM-CSF contains only 2 methionines, while the VSV proteins contain many more (e.g., the M protein contains 12 methionines). When corrected for the reduced methionine content, our results indicate that GM-CSF is expressed at levels similar to those of other VSV proteins. The expression of GM-CSF in infected cells was also confirmed by immunofluorescence microscopy using a PE-labeled antibody to GM-CSF (Fig. 1C). We observed a bright reticular pattern of staining consistent with GM-CSF localization in the endoplasmic reticulum, the localization expected for a secreted protein. Control cells infected with rVSV showed no detectable staining with this antibody (not shown).

Finally, we directly quantitated the production of GM-CSF using an ELISA, which confirmed the high-level production. Eight hours after the infection of 10^6 BHK cells with VSV-GMCSF1, we found a total of 56 ng GM-CSF in the medium and 322 ng in the cell lysate. Control VSV-EGFP1-infected cells made no detectable GM-CSF.

Control VSV expressing EGFP from gene position 1. To generate a control virus expressing a gene of about the same size as GM-CSF, we also constructed a plasmid expressing the 0.7-kb EGFP gene from position 1 of the VSV genome (pVSV1XN-EGFP) and used it to recover VSV-EGFP1. Abundant EGFP expression by this virus was observed by fluorescence microscopy of infected cells (not shown). Recombinant VSVs typically grow to normal titers (>10^8 PFU/ml) even with extra genes inserted at downstream positions in the VSV genome (11). We observed that the recombinant VSVs expressing EGFP or GM-CSF from the first position both grew to lower titers than rVSV lacking an inserted gene. The lower titers of both recombinants are presumably due to the insertion of a foreign gene in the first position, which causes an attenuation of transcription of all downstream genes. To analyze virus production in more detail, we created a one-step growth curve (Fig. 2). We noted that both VSV-EGFP1 and VSV-GMCSF1 grew to lower titers than rVSV lacking any insert.
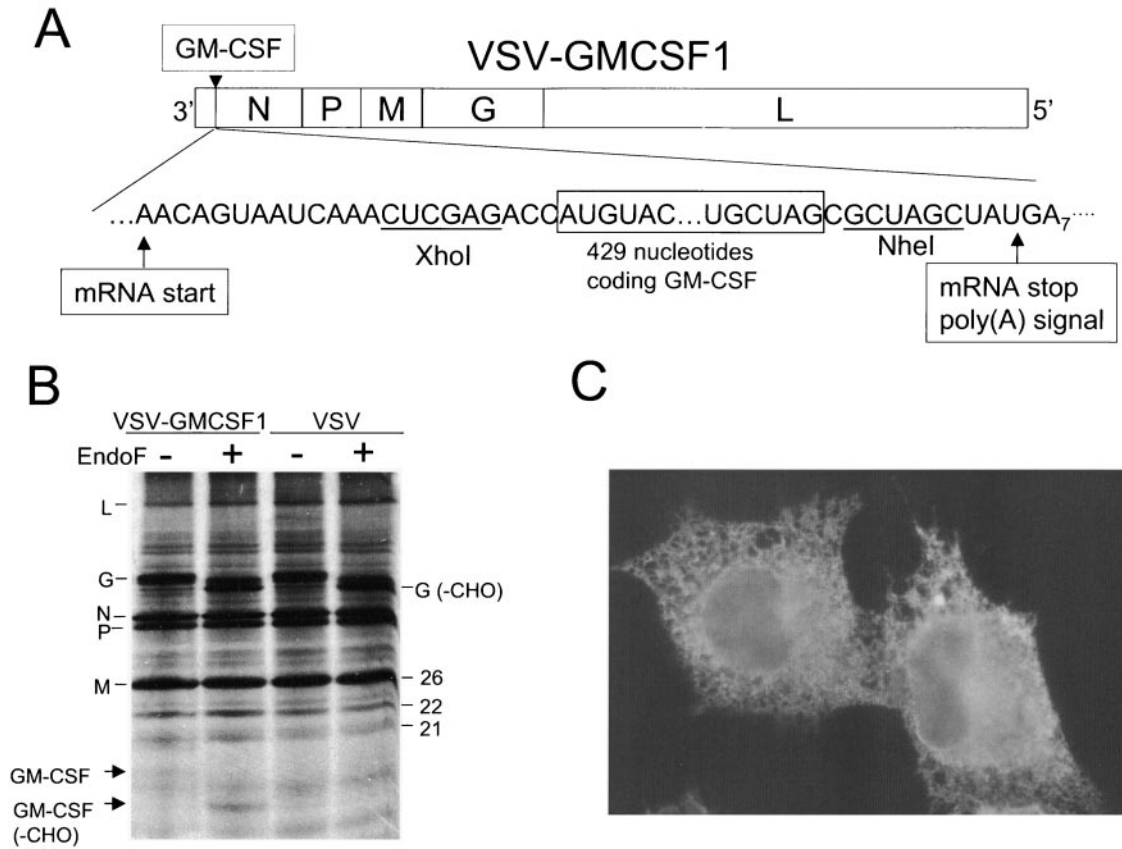
FIG. 1. Recombinant VSV genome and protein expression. Panel A is a diagram showing the gene order of the VSV-GMCSF1 recombinant. The gene order is shown in the 3′-5′ direction of transcription on the negative-strand RNA genome. The GM-CSF gene insertion site and flanking nucleotides, including the transcription and translation start and stop sites, are indicated. Restriction enzyme sites used for cloning the GM-CSF gene at the DNA stage are also indicated. All sequences are shown in the positive (antigenome) sense for clarity. Panel B shows an SDS-PAGE (15% acrylamide) gel containing lysates of BHK cells infected with the indicated viruses and labeled with [^{35}S]methionine. The gel image was collected by autoradiography on X-ray film. Panel C shows an immunofluorescence image of BHK cells infected with VSV-GMCSF1. Cells were infected for 4 h, fixed, permeabilized, and stained with a PE-labeled monoclonal antibody recognizing mGM-CSF. Cells were photographed using a Nikon fluorescence microscope with a 60× Planapochromat objective and a SPOT digital camera.

Recombinant VSV expressing GM-CSF is attenuated for pathogenesis in vivo. Mice infected intranasally with rVSV typically lose weight for 3 to 4 days following infection and then recover to their preinfection weight by about 2 weeks postinfection. The amount and kinetics of weight loss are a sensitive measure of viral pathogenesis, with more attenuated viruses causing less prolonged and less severe weight loss (29). To determine if the viruses expressing GM-CSF or EGFP were attenuated for pathogenesis in mice, we infected groups of 8-week-old C57BL/6 mice intranasally with rVSV, VSV-EGFP1, or VSV-GMCSF1. While all mice survived infection with all the viruses tested, mice infected with rVSV lost an average of 12.8% ± 1.4% of their preinfection body weight by day 3 postvaccination and then began to recover (Fig. 3). Weight loss in mice infected with VSV-EGFP1 was indistinguishable from that in rVSV-infected animals (12.2% ± 1.8% by day 3), indicating that simply inserting a gene into the first position does not have a significant effect on pathogenesis. In contrast, mice infected with VSV-GMCSF1 lost only 7.4% ± 0.9% of their initial body weight, indicating a loss of pathogenesis related to the expression of GM-CSF.
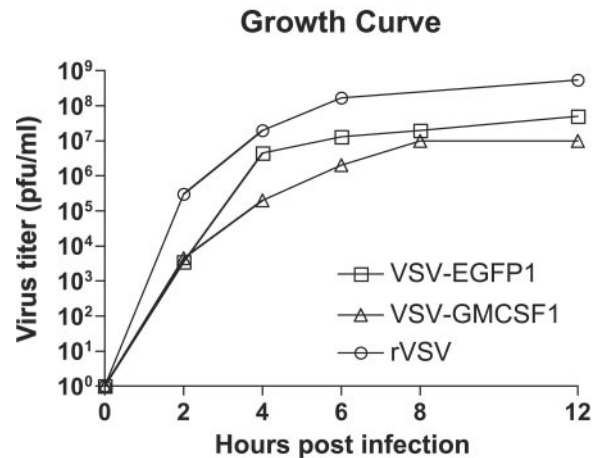

FIG. 2. One-step growth curves for recombinant VSVs. BHK cells (2×10^6) were infected with rVSV (open circles), VSV-EGFP1 (open squares), or VSV-GMCSF1 (open triangles) at an MOI of 10. Viruses were adsorbed to the cells for 30 min, and the cells were then washed to remove input virus and returned to DMEM with 5% fetal bovine serum. Supernatant samples were collected at the indicated times postinfection, kept on ice, and titrated by plaque assays on BHK cells.
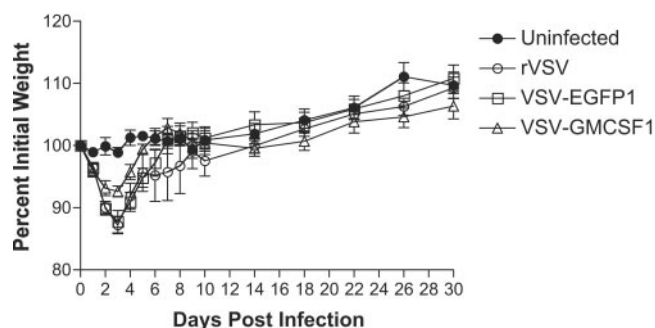
FIG. 3. Pathogenesis measured by weight loss after immunization. Seven-week-old female C57BL/6 mice were immunized intranasally with 5×10^5 PFU wild-type rVSV (open circles), VSV-EGFP1 (open squares), or VSV-GMCSF1 (open triangles). Control mice were sham immunized with sterile DMEM (filled circles). Mice were weighed daily after immunization on day 0. The graph represents average percentages of preimmunization body weights $\pm$ standard errors of the means (SEM) for a minimum of six mice per group.

Replication and spread of VSV-GMCSF1 are significantly attenuated in vivo. After intranasal immunization with rVSV, the virus can typically be recovered from the blood as well as from lung and liver homogenates for up to 3 days after infection (28). Peak titers are usually recovered at 24 h postinfection, and the virus is usually cleared by 4 to 5 days postinfection. To examine the attenuated phenotype of the VSV-GMCSF1 virus in more detail, we examined the kinetics of rVSV, VSV-GMCSF1, and VSV-EGFP1 virus propagation in mice. Mice infected intranasally with 5×10^5 PFU of rVSV had high virus titers in the lungs at 24 h postinfection (2.7×10^5 PFU/g) (Table 1). Mice infected with VSV-EGFP1 had virus titers in the lungs identical to those in mice infected with wild-type virus (Table 1). In contrast, mice infected with VSV-GMCSF1 had 44-fold lower titers in the lungs than the other two groups (6.2×10^3 PFU/g) (Table 1). Virus titers obtained from the plasma and liver followed the same general pattern, with VSV-GMCSF1 reaching significantly lower titers than rVSV or VSV-EGFP1 in the plasma and not replicating to detectable titers in the liver. Note that all mice infected with rVSV or VSV-EGFP1 had detectable plasma titers ($n = 3$ and 7, respectively), while only 4/7 mice infected with VSV-GMCSF1 had measurable viremia. Similarly, 5/6 mice infected with rVSV and 4/6 mice infected with VSV-EGFP1 had detectable titers in the liver at 24 h, while 0/6 mice infected with VSV-GMCSF1 had detectable titers in the liver. We conclude that VSV-GMCSF1 grows to much lower titers in the lungs of infected animals, spreads much less efficiently to organs beyond the lung, and is cleared more rapidly than rVSV or VSV-EGFP1 (Table 1). This re-

duced replication and dissemination of VSV-GMCSF1 almost certainly account for the attenuation of pathogenesis in vivo (Fig. 3).

Primary CD8 T-cell responses to VSV-GMCSF1 are not affected by viral attenuation. To determine if the CD8 T-cell responses to VSV were affected by the attenuation of pathogenesis and replication in vivo, we compared the CD8 T-cell responses elicited by the VSV N protein following intranasal immunization with those elicited by either VSV-EGFP1 or VSV-GMCSF1. Antigen-specific CD8 T cells were identified as cells binding an MHC class I tetramer specific for the VSV N peptide N-RGYVYQGL-C (18, 38). Antigen-specific, activated CD8 T cells were identified based on tetramer binding and downregulation of CD62L. CD62L is a lymphoid homing receptor that is down-regulated upon T-cell activation (20). Peak levels of anti-N CD8 T cells are present at 8 days postimmunization (17). At this time, animals infected with either virus produced high and equivalent percentages of VSV N-specific CD8 T cells in the spleen ($16.1\% \pm 1.9\%$ for VSV-EGFP1 and $16.8\% \pm 2.1\%$ for VSV-GMCSF1; Fig. 4A and C) and the lungs ($26.8\% \pm 5.1\%$ for VSV-EGFP1 and $29.2\% \pm 1.4\%$ for VSV-GMCSF1; Fig. 4B and D). We obtained the same result when the vectors were delivered intramuscularly (Fig. 4E and F). The generation of equivalent responses by both vectors after intranasal delivery was unexpected, as we have previously observed that rVSVs attenuated for growth by truncation of the G cytoplasmic tail generate much lower CD8 T-cell responses when given intranasally (25). For these viruses, the reduction in immune responses correlated directly with the extent of reduction in virus replication. It therefore seemed likely that the expression of GM-CSF was acting to reduce virus replication while at the same time enhancing immune responses to the virus.

Memory and recall CD8 T-cell responses to VSV N are increased after immunization with VSV-GMCSF1. We also assessed memory and recall CD8 T-cell responses to VSV N following immunization with VSV-GMCSF1 and VSV-EGFP1. We define tetramer-positive CD8 T cells present in mice at 30 days postinfection as memory cells because this population remains stable thereafter and can be recalled rapidly upon boosting (7, 10). In mice immunized with VSV-EGFP1, this memory population constituted $1.03\% \pm 0.2\%$ and $16.3\% \pm 2.7\%$ of the CD8$^+$ T cells in the spleen and lungs, respectively (Fig. 4G and H). In mice immunized with VSV-GMCSF1, there were equivalent or increased memory populations, with $1.5\% \pm 0.2\%$ and $28.2\% \pm 5.4\%$ tetramer-positive CD8 T cells in the spleen and lungs, respectively.

To assess the capacity of these cells to reexpand in vivo, we boosted mice from both groups with a recombinant vaccinia

TABLE 1. Virus titers in lungs, plasma, and liver at 24 and 72 h postinfection

Virus	Titer at 24 h postinfection			Titer at 72 h postinfection		
	Lungs[a]	Plasma[b]	Liver[a]	Lungs[a]	Plasma[b]	Liver[a]
rVSV	2.5×10^5	2.6×10^4	6.5×10^4	3.0×10^2	0	0
VSV-EGFP1	2.5×10^5	4.0×10^3	8.4×10^3	1.2×10^3	0	0
VSV-GMCSF1	6.2×10^3	1.2×10^3	0	0	0	0

[a] Titers are expressed as PFU/g.
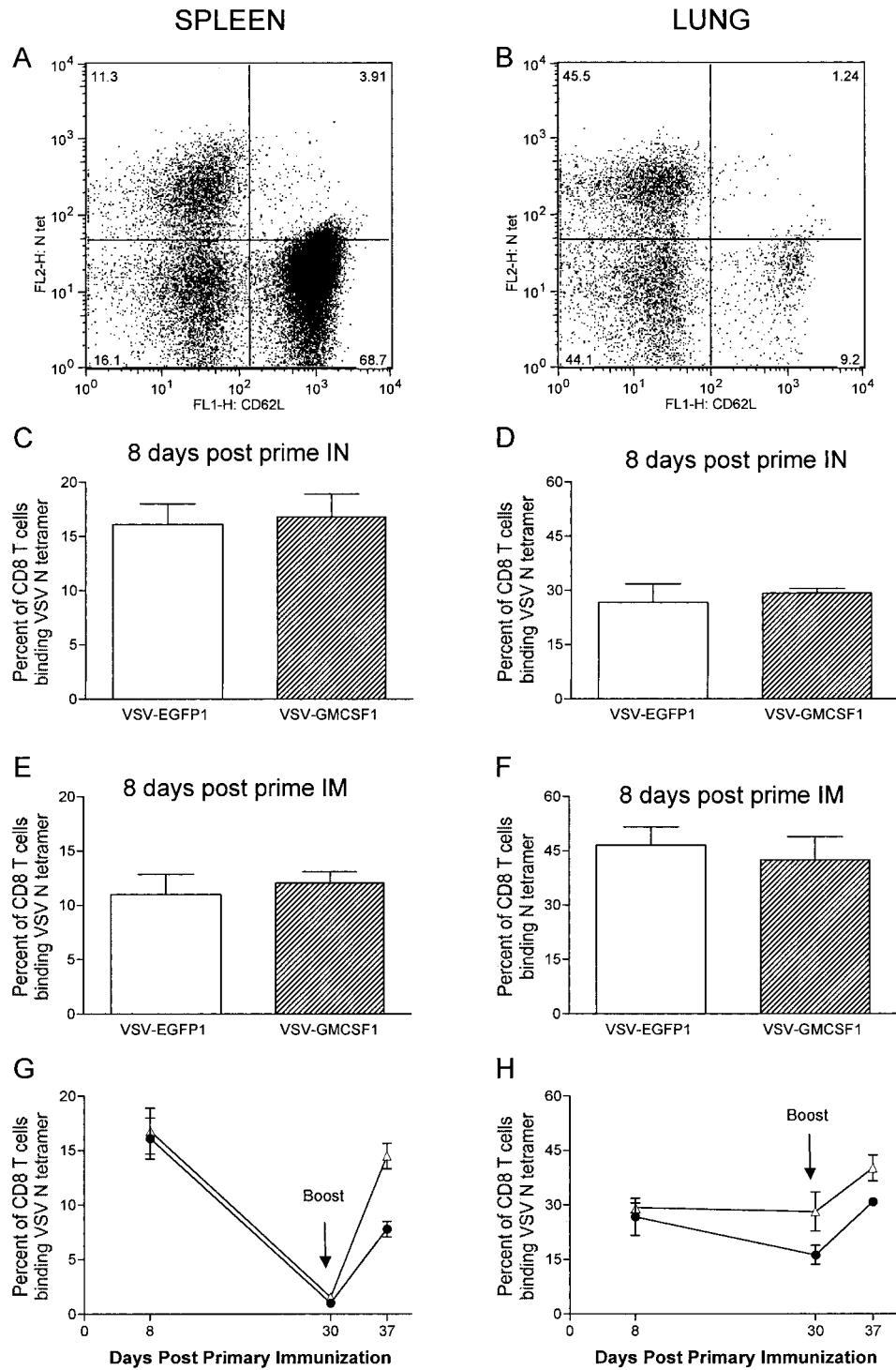[b] Titers are expressed as PFU/ml.

SPLEEN

LUNG

FIG. 4. CD8 T-cell responses to VSV N protein after intranasal and intramuscular immunization. Mice were immunized intranasally (IN) (C, D, G, and H) or intramuscularly (IM) (A, B, E, and F) with 5×10^5 PFU VSV-EGFP1 (open bars or solid circles) or VSV-GMCSF1 (striped bars or open triangles). CD8 T-cell responses to VSV N were analyzed by MHC class I tetramer staining at 8 days post-primary infection (A to H), at 30 days post-primary infection (G and H), or 7 days after the indicated booster with 1×10^5 PFU vaccinia virus (v38) expressing VSV N (G and H). CD8 T cells were isolated from spleens (A, C, E, and G) and lungs (B, D, F, and H) of infected mice. Bars or points represent mean percentages of tetramer-positive CD62L^{lo} CD8 T cells $\pm$ SEM.
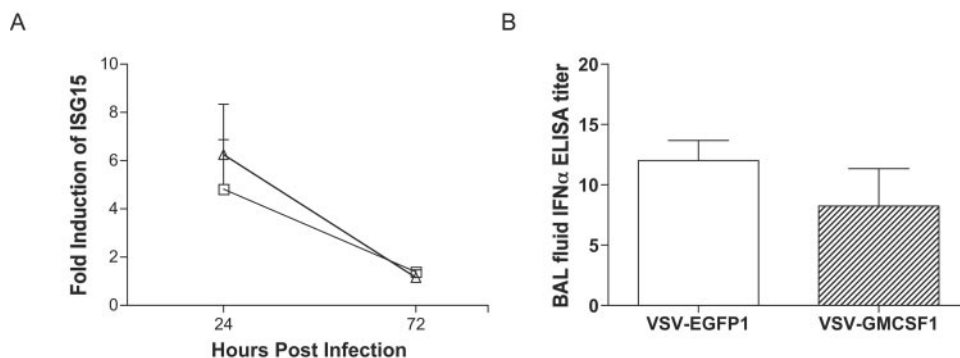
FIG. 5. IFN-α/β responses do not correlate with attenuation of viral replication in the lungs. Seven-week-old female C57BL/6 mice were immunized intranasally with 5×10^5 PFU VSV-EGFP1 (open squares or open bars) or VSV-GMCSF1 (open triangles or striped bars). Whole lung tissue or BAL fluid was collected from mice 24 or 72 h after infection. IFN-α was detected either indirectly (via RT-PCR for IFN-α-responsive gene expression) (A) or directly (via IFN-α ELISA) (B). The IFN-α concentration in BAL fluid (B) was analyzed at 24 h postinfection. Graphs reflect averages of induction of ISG15 (A) or average IFN-α concentrations (B) ± SEM.

virus (v38) expressing the VSV N protein (16). We then analyzed CD8 T-cell responses by using the N tetramer assay 7 days after the booster. We found that mice primed with VSV-GMCSF1 showed a considerably larger expansion of T cells in both the spleen and lungs following the booster. Mice primed with VSV-EGFP1 had 7.8% ± 0.7% and 30.9% ± 1.1% tetramer-positive CD8 T cells in the spleen and lungs, respectively, while mice primed with VSV-GMCSF1 had 14.5% ± 1.2% and 40.2% ± 3.6% tetramer-positive CD8 T cells in the spleen and lungs, respectively (Fig. 4G and H). This represents a true recall response, as naïve mice primed with the boosting virus had only 2.0% ± 0.3% and 3.0% ± 0.8% tetramer-positive CD8 T cells in the spleen and lungs, respectively (data not shown). Our results indicate that the effect of GM-CSF expression by VSV is not restricted to the acute phase of the infection but also enhances CD8 T-cell long-term memory and recall responses.

Neutralizing antibody responses to VSV are not affected by attenuation due to GM-CSF. We next determined if the reduced replication of VSV-GMCSF1 in vivo affected the generation of an anti-VSV neutralizing antibody (NAb) response. Mice were immunized intranasally with either VSV-EGFP1 or VSV-GMCSF1 and then bled 30 days later. NAb titers (representing 100% neutralization of virus) were analyzed by endpoint dilutions of sera, using serial twofold dilutions (32). Mice in both immunization groups developed VSV NAb, and the average titers for VSV-EGFP1- and VSV-GMCSF1-immunized mice were not significantly different (3,413 ± 853 and 2,560 ± 0, respectively).

Attenuation of VSV-GMCSF is not explained by enhanced induction of interferons. VSV replication is very sensitive to

inhibition by both IFN-α/β and IFN-γ (4, 19, 21, 37). We therefore considered the possibility that the replication and dissemination of VSV-GMCSF1 in vivo might be reduced because of increased IFN-α/β and IFN-γ responses to this virus. While there is no presently known direct connection between the production of GM-CSF and IFNs, it seemed likely that the activation of macrophages or other professional APC by GM-CSF could lead to a more efficient antiviral response through the production of interferons.

The induction of genes activated by the presence of IFN is a very sensitive indicator of the level of IFN production. To test the model that enhanced production of IFN-α might be responsible for the rapid control of VSV-GMCSF1 replication, we assayed the induction of two IFN-α/β-inducible genes in the lungs. We prepared cDNAs from whole lung homogenates of mice immunized intranasally with either VSV-EGFP1 or VSV-GMCSF1 and compared the levels of gene expression using real-time RT-PCR. We chose to analyze the expression of two representative IFN-inducible genes (interferon-stimulated gene 15 [ISG15] and the 2′,5′-oligoadenylate synthase [OAS] gene). We found that intranasal infection with either VSV-EGFP1 or VSV-GMCSF1 generated a five- to sixfold induction of these genes in the lungs at 24 h postinfection. By 72 h postinfection, the expression of these genes had returned to background levels (Fig. 5A and Table 2). OAS upregulation followed the same pattern as that for ISG15 (data not shown).

In order to directly quantify IFN-α production, we assayed BAL fluid for the presence of IFN-α at 24 h postinfection. Consistent with the RT-PCR analysis, we found similar levels of IFN-α production in animals infected with VSV-GMCSF1 compared to those in animals infected with VSV-EGFP1

TABLE 2. Induction of interferons and interferon-responsive genes[a]

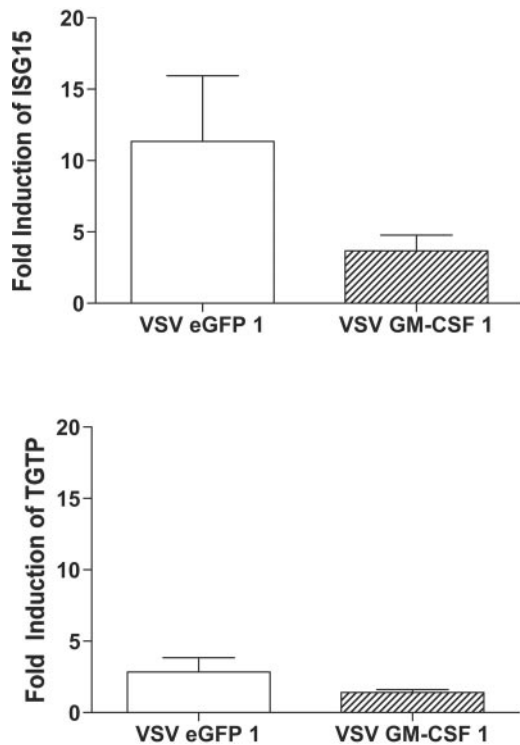| Virus	Fold induction of IFN-α responsive gene ISG15		IFN-α concn in BAL fluid (pg/ml)	Fold induction of IFN-responsive genes by BAL fluid	
	24 h postinfection	72 h postinfection	24 h postinfection	IFN-α (ISG15)	IFN-γ (TGTP)
VSV-EGFP1	4.8 ± 2.0	No induction	12.0 ± 1.7	11.4 ± 4.6	2.8 ± 1.0
VSV-GMCSF1	6.3 ± 2.1	No induction	8.3 ± 3.1	3.7 ± 1.1	No induction

[a] Data are means ± SEM.

FIG. 6. IFN-γ production does not correlate with attenuation of viral replication in the lung. Seven-week-old female C57BL/6 mice were immunized intranasally with 5×10^5 PFU VSV-EGFP1 (open bars) or VSV-GMCSF1 (striped bars). BAL fluid was collected at 24 h postimmunization. After 24 h, hepatocytes were collected and analyzed via RT-PCR for the induction of IFN-α- or IFN-γ-responsive genes (upper panel, ISG15; lower panel, TGTP). Graphs represent averages of induction of these genes ± SEM.

(Fig. 5B and Table 2). Viral titers peaked in the lungs at 24 h postinfection, with VSV-EGFP1-infected animals having, on average, at least 10-fold higher titers than VSV-GMCSF1-infected animals (Table 1). These data demonstrate that the

difference in virus titers cannot be explained by an increased induction of IFN-α production by VSV-GMCSF1.

VSV replication is also sensitive to IFN-γ. To determine whether enhanced IFN-γ production might be responsible for the control of VSV replication in the lungs, we assayed BAL fluid for the ability to induce upregulation of the IFN-γ-inducible gene TGTP in a hepatocyte cell line. This cell line was chosen for its sensitivity to IFN and its high level of IFN-induced gene expression. As a control, we measured the induction of the IFN-α-inducible gene ISG15 concurrently. Consistent with the results obtained with the IFN-α ELISA of BAL fluid, BAL fluid from mice infected with VSV-EGFP1 induced more upregulation of IFN-α-responsive ISG15 than BAL fluid from mice infected with VSV-GMCSF1 (11-fold versus 4-fold) (Fig. 6A and Table 2). Interestingly, the IFN-γ-inducible gene TGTP was only slightly upregulated in VSV-EGFP1-infected mice (threefold), while no induction was observed in VSV-GMCSF1-infected mice (Fig. 6B and Table 2). We believe this represents the presence of low levels of IFN-α and IFN-γ, as BAL fluid collected from uninfected animals induced no ISG15 or TGTP expression at all. In hepatocytes treated with purified IFN-α or IFN-γ as a positive control, ISG15 and TGTP were induced at high levels (71-fold and 1,453-fold, respectively). Together, these data demonstrate that neither increased IFN-α/β nor IFN-γ induction explains the inhibition of VSV-GMCSF1 replication in the lungs.

Enhanced recruitment of macrophages may restrict replication of VSV-GMCSF1. The primary function of GM-CSF is to stimulate the maturation and recruitment of monocytes and other antigen-presenting cells. We examined the cells present in the BAL fluid of mice infected intranasally to see whether macrophages were recruited more efficiently to the lungs of mice infected with VSV-GMCSF1. At 24 h postinfection, dendritic cells (CD11b^lo CD11c^hi) were present in the BAL fluid of all immunized mice (Fig. 7B and C), but their levels did not appear different from those present in uninfected controls (Fig. 7A). In contrast, a large population of macrophages (CD11b^hi CD11c^lo) not present in uninfected animals was recruited to the lungs of some immunized animals by 24 h postin-
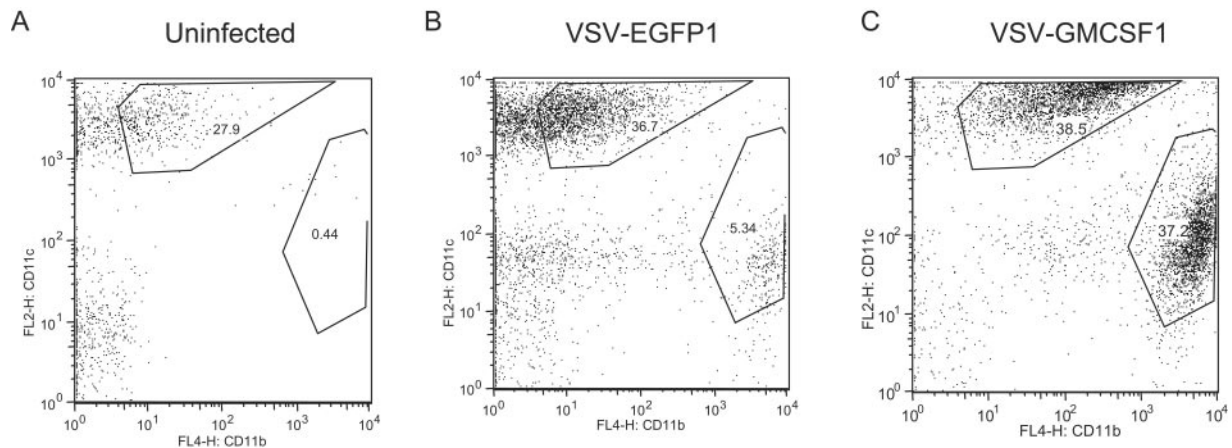

FIG. 7. VSV-GMCSF1 induces enhanced recruitment of macrophages to the lungs after intranasal immunization. Seven-week-old female C57BL/6 mice were either sham immunized (A) or immunized intranasally with 5×10^5 PFU VSV-EGFP1 (B) or VSV-GMCSF1 (C). BAL fluid was collected 24 h after infection. Cells were separated from the BAL fluid and immediately stained for CD11b and CD11c expression.

fection (Fig. 7A to C). The absolute number of cells in the BAL fluid varied considerably between animals. In order to quantify and compare differences between animals, we calculated the ratio of dendritic cells to macrophages for each individual and compared these numbers. In the uninfected mice, there were more dendritic cells than macrophages, with the average ratio of dendritic cells to macrophages being 44.4. Mice infected with VSV-EGFP1 ($n = 8$) generally were similar to uninfected animals, having an average ratio of 22.0. In contrast, mice infected with VSV-GMCSF1 ($n = 8$) typically had a much greater proportion of macrophages in the BAL fluid, with an average ratio of 2.6. These results suggest that the inclusion of GM-CSF in the viral vector results in greater recruitment of macrophages to the lungs following VSV infection.

DISCUSSION

Experimental vaccines based on the recombinant VSV platform induce strong cellular and humoral immune responses and solid protection in animal models of several human viral diseases (27, 29, 30, 33). Although no vector-associated pathogenesis has been detected in more than 100 nonhuman primates given VSV vectors by the intranasal, oral, and intramuscular routes (5, 27, 31), it is likely that the introduction of specific attenuating mutations will be required before replication-competent VSV vectors will be approved for large-scale use in humans. Accordingly, our laboratory has focused on methods for VSV vector attenuation without a loss of immunogenicity. We have found that VSVs attenuated for replication or defective VSV vectors capable of only one round of replication are also attenuated for immunogenicity when given by the intranasal route, a noninvasive route that would be very convenient for mass vaccination. These attenuated vectors still induce strong immune responses after intramuscular or intraperitoneal vaccination (Publicover et al., manuscript submitted).

We undertook the current study to determine if we could design a replicating rVSV vector that would induce strong or enhanced immune responses when delivered by the noninvasive intranasal route but be attenuated in terms of host pathogenesis. The virus designed employed a novel VSV vector that allowed murine GM-CSF expression from the first position in the VSV genome, upstream of the VSV N gene. This placement of the foreign gene allows for maximal mRNA and protein expression while also preventing the loss of foreign gene expression through mutations eliminating the upstream transcription stop codon. Such a mutation generates a bicistronic mRNA and prevents translation of the downstream cistron. Such a mechanism was shown previously to result in the rapid elimination of expression of a foreign gene inhibiting VSV replication which was placed between the VSV G and L genes (26). Because there is no gene upstream of the GM-CSF gene in VSV-GMCSF1, protein expression from the gene cannot be lost by such a mechanism.

We demonstrate here that VSV-GMCSF1, expressing murine GM-CSF, is highly attenuated in terms of viral replication and dissemination in vivo. Importantly, however, cellular and humoral responses to this virus were not decreased, and long-term memory CD8 T-cell responses were enhanced. Additionally, primary CD8 T-cell responses to VSV-GMCSF1 were nearly equivalent in mice immunized intranasally and intramuscularly. These characteristics make this virus an excellent candidate for further vaccine development.

We do not know the mechanism of attenuation of VSV-GMCSF1 spread and pathogenesis in mice. One possibility is that the GM-CSF produced during infection acts directly on neighboring cells, rendering them resistant to infection by upregulating "antiviral response" genes such as those encoding interferons. GM-CSF could also act indirectly, by recruiting and/or activating pulmonary APC that produce cytokines that then lead to a reduced infectivity of neighboring cells. Finally, macrophages, dendritic cells, or other cells recruited by GM-CSF might directly kill and/or phagocytose VSV-infected cells, leading to a more efficient containment of infection. Direct effects of GM-CSF on neighboring cells are unlikely, as it has been reported (13) that preincubation of murine macrophages with GM-CSF did not affect VSV infection of these cells, while G-CSF did render them resistant to infection. Our data are consistent with the recruitment hypothesis, as mice infected with VSV-GMCSF1 showed a rapid recruitment of macrophages to the lungs after immunization. This recruitment could also explain the enhanced immune responses observed. If VSV-GMCSF1 were to recruit more professional APC to the site of infection, this would likely lead to better antigen presentation and stronger T-cell responses.

Bukreyev et al. (3) reported that a recombinant respiratory syncytial virus (rRSV) expressing murine GM-CSF (rRSV/mGM-CSF) was attenuated for replication in mice. In their study, the attenuation of rRSV/mGM-CSF was attributed to a greater recruitment of pulmonary antigen-presenting cells, which they proposed resulted in the production of more IFN-γ by pulmonary T cells, leading to a reduction in viral replication. That study showed a significant increase in IFN-γ mRNA in the lungs of rRSV/mGM-CSF-infected mice, which presumably resulted in increased IFN-γ production. The VSV-GMCSF1 virus described here was also greatly attenuated for replication in the lungs and elsewhere compared to a control VSV-EGFP1 virus. Although the control virus did induce IFN-γ in the lungs of infected mice, VSV-GMCSF1 did not. Similarly, the VSV-GMCSF1 virus induced less IFN-α than VSV-EGFP1. Thus, increased interferon production does not explain the attenuation of pVSV-GMCSF1. The generally reduced levels of IFN expression and gene induction by VSV-GMCSF1 are probably due to the lower level of virus replication. Although the attenuation of both VSV-GMCSF1 and rRSV/mGM-CSF correlates with the increased ability of these viruses to recruit pulmonary APC, the effector molecules produced by these APC or the T cells they prime may be different. Also, the changes in immune responses to the viruses due to GM-CSF production were somewhat different in the two systems. The CD8 T-cell response to RSV expressing GM-CSF was reduced, while the response to VSV-GMCSF1 was not reduced, and memory and recall responses to this virus were enhanced. The differences between the responses in the two viral systems could be related to the relatively poor replication of human RSV in mice and its lack of pathogenesis or to some other factor, such as the different strategies employed by these viruses in countering host immune responses.

Given the decreased pathogenesis and increased memory CD8 CTL responses generated by VSV-GMCSF1, this virus

clearly warrants further development as a vaccine platform. The development of high levels of memory CD8 T-cell responses is a major goal in vaccine research, especially in the AIDS vaccine field. While plasmid delivery of GM-CSF as a vaccine adjuvant was promising in mice, the responses to plasmid-expressed GM-CSF in humans and monkeys have been disappointing (15, 39). This may be due to the low immunogenicity of DNA vectors in monkeys and humans. The placement of GM-CSF in a highly immunogenic viral vector such as rVSV, which is then attenuated in terms of host pathology, may be an ideal balance between immunogenicity and pathogenicity that will facilitate immune responses to vaccination.

REFERENCES

1. Akagawa, K. S., K. Kamoshita, and T. Tokunaga. 1988. Effects of granulocyte-macrophage colony-stimulating factor and colony-stimulating factor-1 on the proliferation and differentiation of murine alveolar macrophages. J. Immunol. 141:3383–3390.
2. Barouch, D. H., S. Santra, K. Tenner-Racz, P. Racz, M. J. Kuroda, J. E. Schmitz, S. S. Jackson, M. A. Lifton, D. C. Freed, H. C. Perry, M. E. Davies, J. W. Shiver, and N. L. Letvin. 2002. Potent CD4+ T cell responses elicited by a bicistronic HIV-1 DNA vaccine expressing gp120 and GM-CSF. J. Immunol. 168:562–568.
3. Bukreyev, A., I. M. Belyakov, J. A. Berzofsky, B. R. Murphy, and P. L. Collins. 2001. Granulocyte-macrophage colony-stimulating factor expressed by recombinant respiratory syncytial virus attenuates viral replication and increases the level of pulmonary antigen-presenting cells. J. Virol. 75:12128–12140.
4. Chesler, D. A., C. Dodard, G. Y. Lee, D. E. Levy, and C. S. Reiss. 2004. Interferon-gamma-induced inhibition of neuronal vesicular stomatitis virus infection is STAT1 dependent. J. Neurovirol. 10:57–63.
5. Egan, M. A., S. Y. Chong, N. F. Rose, S. Megati, K. J. Lopez, E. B. Schadeck, J. E. Johnson, A. Masood, P. Piacente, R. E. Druilhet, P. W. Barras, D. L. Hasselschwert, P. Reilly, E. M. Mishkin, D. C. Montefiori, M. G. Lewis, D. K. Clarke, R. M. Hendry, P. A. Marx, J. H. Eldridge, S. A. Udem, Z. R. Israel, and J. K. Rose. 2004. Immunogenicity of attenuated vesicular stomatitis virus vectors expressing HIV type 1 Env and SIV Gag proteins: comparison of intranasal and intramuscular vaccination routes. AIDS Res. Hum. Retrovir. 20:989–1004.
6. Haglund, K., I. Leiner, K. Kerksiek, L. Buonocore, E. Pamer, and J. K. Rose. 2002. High-level primary CD8+ T-cell response to human immunodeficiency virus type 1 Gag and Env generated by vaccination with recombinant vesicular stomatitis viruses. J. Virol. 76:2730–2738.
7. Haglund, K., I. Leiner, K. Kerksiek, L. Buonocore, E. Pamer, and J. K. Rose. 2002. Robust recall and long-term memory T-cell responses induced by prime-boost regimens with heterologous live viral vectors expressing human immunodeficiency virus type 1 Gag and Env proteins. J. Virol. 76:7506–7517.
8. Hamilton, J. A., and G. P. Anderson. 2004. GM-CSF biology. Growth Factors 22:225–231.
9. Iverson, L. E., and J. K. Rose. 1981. Localized attenuation and discontinuous synthesis during vesicular stomatitis virus transcription. Cell 23:477–484.
10. Kim, S. K., K. S. Schluns, and L. Lefrancois. 1999. Induction and visualization of mucosal memory CD8 T cells following systemic virus infection. J. Immunol. 163:4125–4132.
11. Kretzschmar, E., L. Buonocore, M. J. Schnell, and J. K. Rose. 1997. High-efficiency incorporation of functional influenza virus glycoproteins into recombinant vesicular stomatitis viruses. J. Virol. 71:5982–5989.
12. Lawson, N. D., E. A. Stillman, M. A. Whitt, and J. K. Rose. 1995. Recombinant vesicular stomatitis viruses from DNA. Proc. Natl. Acad. Sci. USA 92:4477–4481.
13. Lee, M. T., and M. K. Warren. 1987. CSF-1-induced resistance to viral infection in murine macrophages. J. Immunol. 138:3019–3022.
14. Lund, J. M., L. Alexopoulou, A. Sato, M. Karow, N. C. Adams, N. W. Gale, A. Iwasaki, and R. A. Flavell. 2004. Recognition of single-stranded RNA viruses by Toll-like receptor 7. Proc. Natl. Acad. Sci. USA 101:5598–5603.
15. MacGregor, R. R., J. D. Boyer, K. E. Ugen, K. E. Lacy, S. J. Gluckman, M. L. Bagarazzi, M. A. Chattergoon, Y. Baine, T. J. Higgins, R. B. Ciccarelli, L. R. Coney, R. S. Ginsberg, and D. B. Weiner. 1998. First human trial of a DNA-based vaccine for treatment of human immunodeficiency virus type 1 infection: safety and host response. J. Infect. Dis. 178:92–100.
16. Mackett, M., T. Yilma, J. K. Rose, and B. Moss. 1985. Vaccinia virus recombinants: expression of VSV genes and protective immunization of mice and cattle. Science 227:433–435.
17. Marzo, A. L., V. Vezys, K. D. Klonowski, S. J. Lee, G. Muralimohan, M. Moore, D. F. Tough, and L. Lefrancois. 2004. Fully functional memory CD8 T cells in the absence of CD4 T cells. J. Immunol. 173:969–975.
18. Masopust, D., V. Vezys, A. L. Marzo, and L. Lefrancois. 2001. Preferential localization of effector memory cells in nonlymphoid tissue. Science 291:2413–2417.
19. Meraz, M. A., J. M. White, K. C. Sheehan, E. A. Bach, S. J. Rodig, A. S. Dighe, D. H. Kaplan, J. K. Riley, A. C. Greenlund, D. Campbell, K. Carver-Moore, R. N. DuBois, R. Clark, M. Aguet, and R. D. Schreiber. 1996. Targeted disruption of the Stat1 gene in mice reveals unexpected physiologic specificity in the JAK-STAT signaling pathway. Cell 84:431–442.
20. Mueller, C., H. K. Gershenfeld, C. G. Lobe, C. Y. Okada, R. C. Bleackley, and I. L. Weissman. 1988. A high proportion of T lymphocytes that infiltrate H-2-incompatible heart allografts in vivo express genes encoding cytotoxic cell-specific serine proteases, but do not express the MEL-14-defined lymph node homing receptor. J. Exp. Med. 167:1124–1136.
21. Muller, U., U. Steinhoff, L. F. Reis, S. Hemmi, J. Pavlovic, R. M. Zinkernagel, and M. Aguet. 1994. Functional role of type I and type II interferons in antiviral defense. Science 264:1918–1921.
22. Okada, E., S. Sasaki, N. Ishii, I. Aoki, T. Yasuda, K. Nishioka, J. Fukushima, J. Miyazaki, B. Wahren, and K. Okuda. 1997. Intranasal immunization of a DNA vaccine with IL-12- and granulocyte-macrophage colony-stimulating factor (GM-CSF)-expressing plasmids in liposomes induces strong mucosal and cell-mediated immune responses against HIV-1 antigens. J. Immunol. 159:3638–3647.
23. Paine, R., III, A. M. Preston, S. Wilcoxen, H. Jin, B. B. Siu, S. B. Morris, J. A. Reed, G. Ross, J. A. Whitsett, and J. M. Beck. 2000. Granulocyte-macrophage colony-stimulating factor in the innate immune response to Pneumocystis carinii pneumonia in mice. J. Immunol. 164:2602–2609.
24. Pasquetto, V., S. F. Wieland, S. L. Uprichard, M. Tripodi, and F. V. Chisari. 2002. Cytokine-sensitive replication of hepatitis B virus in immortalized mouse hepatocyte cultures. J. Virol. 76:5646–5653.
25. Publicover, J., E. Ramsburg, and J. K. Rose. 2004. Characterization of nonpathogenic, live, viral vaccine vectors inducing potent cellular immune responses. J. Virol. 78:9317–9324.
26. Quinones-Kochs, M. I., M. J. Schnell, L. Buonocore, and J. K. Rose. 2001. Mechanisms of loss of foreign gene expression in recombinant vesicular stomatitis viruses. Virology 287:427–435.
27. Ramsburg, E., N. F. Rose, P. A. Marx, M. Mefford, D. F. Nixon, W. J. Moretto, D. Montefiori, P. Earl, B. Moss, and J. K. Rose. 2004. Highly effective control of an AIDS virus challenge in macaques by using vesicular stomatitis virus and modified vaccinia virus Ankara vaccine vectors in a single-boost protocol. J. Virol. 78:3930–3940.
28. Roberts, A., L. Buonocore, R. Price, J. Forman, and J. K. Rose. 1999. Attenuated vesicular stomatitis viruses as vaccine vectors. J. Virol. 73:3723–3732.
29. Roberts, A., E. Kretzschmar, A. S. Perkins, J. Forman, R. Price, L. Buonocore, Y. Kawaoka, and J. K. Rose. 1998. Vaccination with a recombinant vesicular stomatitis virus expressing an influenza virus hemagglutinin provides complete protection from influenza virus challenge. J. Virol. 72:4704–4711.
30. Roberts, A., J. D. Reuter, J. H. Wilson, S. Baldwin, and J. K. Rose. 2004. Complete protection from papillomavirus challenge after a single vaccination with a vesicular stomatitis virus vector expressing high levels of L1 protein. J. Virol. 78:3196–3199.
31. Rose, N. F., P. A. Marx, A. Luckay, D. F. Nixon, W. J. Moretto, S. M. Donahoe, D. Montefiori, A. Roberts, L. Buonocore, and J. K. Rose. 2001. An effective AIDS vaccine based on live attenuated vesicular stomatitis virus recombinants. Cell 106:539–549.
32. Rose, N. F., A. Roberts, L. Buonocore, and J. K. Rose. 2000. Glycoprotein exchange vectors based on vesicular stomatitis virus allow effective boosting and generation of neutralizing antibodies to a primary isolate of human immunodeficiency virus type 1. J. Virol. 74:10903–10910.
33. Schlereth, B., J. K. Rose, L. Buonocore, V. ter Meulen, and S. Niewiesk. 2000. Successful vaccine-induced seroconversion by single-dose immunization in the presence of measles virus-specific maternal antibodies. J. Virol. 74:4652–4657.
34. Schnell, M. J., L. Buonocore, M. A. Whitt, and J. K. Rose. 1996. The minimal conserved transcription stop-start signal promotes stable expression of a foreign gene in vesicular stomatitis virus. J. Virol. 70:2318–2323.
35. Sedegah, M., W. Weiss, J. B. Sacci, Jr., Y. Charoenvit, R. Hedstrom, K. Gowda, V. F. Majam, J. Tine, S. Kumar, P. Hobart, and S. L. Hoffman. 2000. Improving protective immunity induced by DNA-based immunization: priming with antigen and GM-CSF-encoding plasmid DNA and boosting with antigen-expressing recombinant poxvirus. J. Immunol. 164:5905–5912.
36. Shibata, Y., P. Y. Berclaz, Z. C. Chroneos, M. Yoshida, J. A. Whitsett, and B. C. Trapnell. 2001. GM-CSF regulates alveolar macrophage dif-

ferentiation and innate immunity in the lung through PU.1. Immunity **15:**557–567.

37. **Steinhoff, U., U. Muller, A. Schertler, H. Hengartner, M. Aguet, and R. M. Zinkernagel.** 1995. Antiviral protection by vesicular stomatitis virus-specific antibodies in alpha/beta interferon receptor-deficient mice. J. Virol. **69:** 2153–2158.

38. **Van Bleek, G. M., and S. G. Nathenson.** 1990. Isolation of an endogenously processed immunodominant viral peptide from the class I H-2Kb molecule. Nature **348:**213–216.

39. **Wang, R., D. L. Doolan, T. P. Le, R. C. Hedstrom, K. M. Coonan, Y. Charoenvit, T. R. Jones, P. Hobart, M. Margalith, J. Ng, W. R. Weiss, M. Sedegah, C. de Taisne, J. A. Norman, and S. L. Hoffman.** 1998. Induction of antigen-specific cytotoxic T lymphocytes in humans by a malaria DNA vaccine. Science **282:**476–480.

40. **Weiss, W. R., K. J. Ishii, R. C. Hedstrom, M. Sedegah, M. Ichino, K. Barnhart, D. M. Klinman, and S. L. Hoffman.** 1998. A plasmid encoding murine granulocyte-macrophage colony-stimulating factor increases protection conferred by a malaria DNA vaccine. J. Immunol. **161:**2325–2332.